IOPscience iopscience.iop.org

Home Search Collections Journals About Contact us My IOPscience

Microscopy Studies for the Deep-Anisotropic Etching of (100) Si Wafers

This content has been downloaded from IOPscience. Please scroll down to see the full text.

1992 Jpn. J. Appl. Phys. 31 3489

(http://iopscience.iop.org/1347-4065/31/11R/3489)

View the table of contents for this issue, or go to the journal homepage for more

Download details:

IP Address: 163.152.61.222
This content was downloaded on 19/03/2014 at 07:58

Please note that terms and conditions apply.

Jpn. J. Appl. Phys. Vol. 31 (1992) pp. 3489–3494
Part 1, No. 11, November 1992

Microscopy Studies for the Deep-Anisotropic Etching of (100) Si Wafers

Byeong Kwon JU, Byeoung Ju HA[1], Chul Ju KIM[1],
Myung Hwan OH and Kyun Hyon TCHAH[2]

Division of Applied Science and Engineering, KIST, 39-1, Haweolgog-dong, Seongbuk-gu, Seoul 136-791, Korea
[1]*Department of Electronic Engineering, Seoul City University, Dongdaemun-gu, Seoul 130-743, Korea*
[2]*Department of Electronic Engineering, Korea University, Seongbuk-gu, Seoul 136-701, Korea*

(Received February 25, 1992; accepted for publication August 15, 1992)

Several etching phenomena appeared during the Si membrane process were observed and analyzed. In case of deep etching to above 300 μm depth, the etch-defects existed at the etched surface could be classified into three categories such as hillocks, adhered reaction products and white residues. It was known that the hillocks had a pyramidal shape or trapizoidal hexahedron structures depending on the density and size of the reaction products. Also, the existence of etch-defects and the etch rate distribution over a whole 4-inch wafers were investigated when the surfaces to be etched were downward, upward horizontally and erective for the stirring bar in the solution. As the results, the downward and erected postures were favorable in the etch rate uniformity and the etch-defect removal, respectively.

KEYWORDS: Si deep etching, anisotropic etching, etch-defects, Si membrane

§1. Introduction

The biggest problem in the mass production of Si mechanical sensor including pressure sensor has been lying in the batch fabrication of the thin Si membrane.[1-3] Moreover, as the wafer diameter increases, it becomes more and more difficult to form membranes having a good surface and thickness uniformity over a whole wafer area. And so, 2-inch sized or only $100 \sim 250\,\mu$m thick Si wafers have been mostly employed in the processing of membrane-based sensor until now.

In order to improve such a small scale processing which is not available in the standard IC batch fabrication, several reports have treated a deeper anisotropic etching using a larger-sized wafers.[2-4] But the samples used in those experiments were limited to the range of 3-inch in diameter and 200 μm in etching depth at most.

In this study, we expand the range into a value of 4-inch diameter and above 300 μm etching depth. Then, we investigate the presence of etch-defects, etch rate distribution, and evaluate the applicability of very deep etching to the membrane formation by analyzing the flow patterns of an etching solution in a container.

§2. Experimental Procedures

530 μm thick, 4-inch (100) Si wafers were used. The wafers were wet-oxidized to form 0.2 μm thick SiO_2 film as an etch mask and then, 88 square-shaped oxide windows of 1.7×1.7 mm^2 were opened on the frontside by a photolithography as shown in Fig. 1. The oxide grown on the backside was protected.

Figure 2 shows the apparatus in which the samples were to be etched. The catalyzed EPW solution was employed as an "F etchant" in accordance with the literature.[4,5] The composition was ethylenediamine (E): 1710 m*l*, pyrocatechol (P): 547.2 gr, water (W): 547.2 gr and pyrazine: 10.26 gr. The etching temperature was fixed to 115 ± 0.5°C.

Magnetic stirrer and reflux condenser were installed in the apparatus and the stirring speed was controlled within a range of 300 ± 5 rpm considering the proper rotating force of the solution. N_2 bubbling was avoided because it might disperse the flow patterns of solution. The used "F etch" solution was replaced with new one after that each etching was completed in order to preserve it from the oxidizing or changing in the composition. The etching time was measured from the time when H_2 gas started to evolve from the surface to be etched (in $3\sim5$ min after dipping) indicating the presence of a thin native oxide.[3] Etching was done for 240 min by which it could be supposed that at least 300 μm deep cavities were formed on the patterned surface. When the etching was

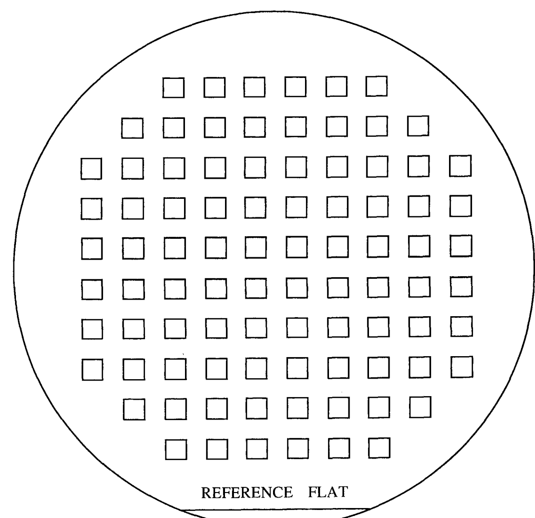

Fig. 1. Patterned wafer before etching.

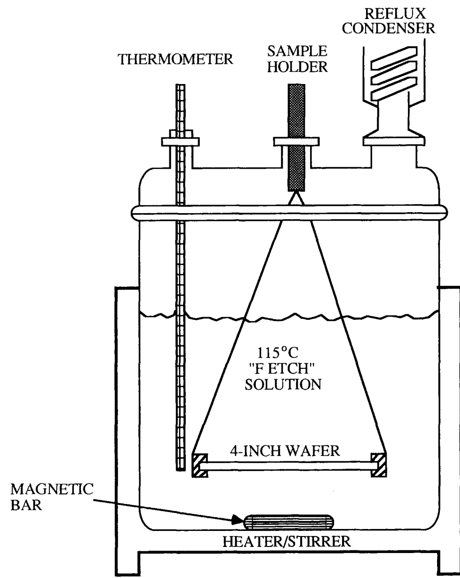

Fig. 2. Schematic drawing of the etching apparatus.

completed the sample was taken out of the solution and immediately rinsed in a 97°C deionized water because some cooled solutions in the etched cavity might be over-saturated, resulting in residue formation.[2)]

The sample postures were emphasized as main variables in this experiment. The series of F1, F2 and F3 were laid each differently on the teflon holder as shown in Fig. 3. We carried out the etching with five wafers per each "F" series and extracted three samples, which showed a nearest one with the average or general tendency in each series. The extracted three samples were named for "sample F1", "sample F2", and "sample F3," respectively.

§3. Results and Discussion

The undesirable effects appeared at the etched surface could almost be classified into three types, as shown in Fig. 4, under optical microscope and they were thought to be hillock clusters, adhered reaction products and white residues, respectively.[2,6-9)]

More than 90% of the etch-defects observed in this experiment had a shape of the hillock clusters like Fig. 4(a) and especially, they were occurred severely for the case of sample F2. They rose convexly near the center of the etched surface, having an area between $2\times2\ \mu m^2 \sim 700\times700\ \mu m^2$ and the height of about $5\sim10\ \mu m$. The SEM photographs for the various hillock clusters were shown in Fig. 5 and these phenomena could be explained through the schematic illustration shown in Fig. 6.[8-10)]

That is, while the etching proceeded, there existed some reaction products considered as a species of silica and evolved H_2 gas in the opened cavity. In case that the cavity was shallow, the by-products were transferred to the outside through the solution flow near the surface. However, in case of deep etching, the trapped-eddy patterns were generated in the cavity and they interrupted the products from being washed out to the outside.[10-12)] Thus, there were a larger amount of micro- or macro-substances in the cavity as the etch depth was increased and these acted as etch masks during further etching. The hillocks generated by the above mechanisms had usually pyramidal shapes composed with four {111} planes as

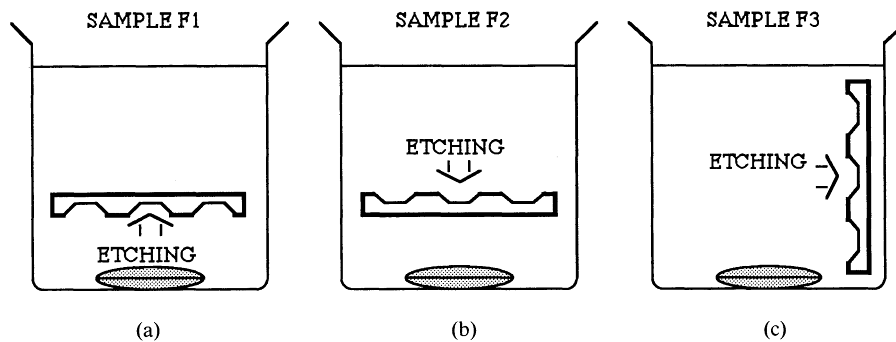

Fig. 3. Etching postures for the smple F1(a), F2(b), and F3(c).

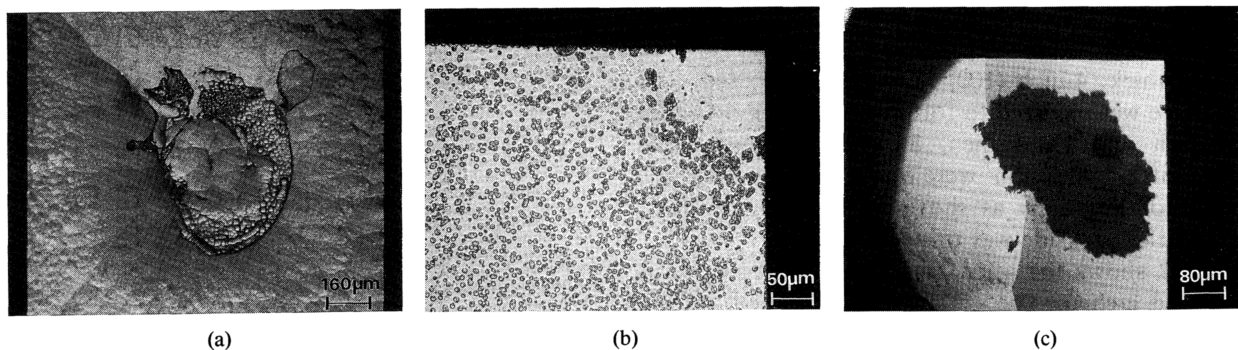

Fig. 4. Three types of the observed etch-defects; hillock clusters (a), adhered reaction products (b), and white residues (c).

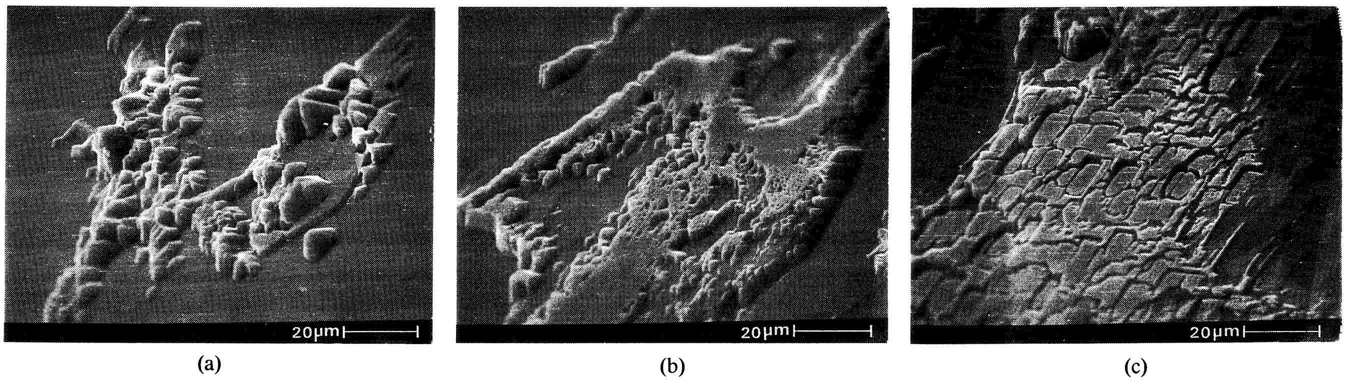

Fig. 5. Various types of hillock clusters; dispersed (a), congregated hillock clusters of pyramidal shape (b), and congregated hillock clusters of hexahedral shape (c).

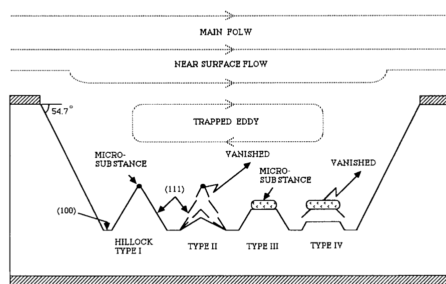

Fig. 6. Schematic illustration about hillock formation model.

shown in Fig. 5(a). But when there were large-sized substances the hillocks would appear like trapizoidal hexagon structures as in the case of Fig. 5(b) and their height was lowered gradually as etching was proceeded like in Fig. 5(c).

Figures 7(a) and 7(b) show magnified features for the case of Figs. 4(b) and 4(c), respectively. It was discovered that about $7\sim8\%$ of the observed defects were similar to the shapes shown in Fig. 7(a) and these types of defects might be due to the reaction products adhered to the surface right before the etching was completed. The phenomena as shown in Fig. 7(b) were almost not discovered except for a couple of etched cavities. Therefore, it was inferred that we could avoid the local over-saturation of dissolved Si atoms through the good controlling of the conditions of solutions during etching and rinsing of the etched surface in a hot water. The residues looked like snowflakes and were ascertained as a Si–N–O compound mixed with a small amount of H and C through an IR absorption spectra shown in Fig. 8, which was a similar result to the one obtained by Wu *et al.*[2]

Next, as shown in Fig. 9, we mapped out the distribution of etch-defects and etch rate on the whole wafers in order to compare the influences of sample postures on the etching characteristics. The postures of samples in the solutions were described in the previous section. We measure the etch rate by observation of cross-section using a 500X magnified microscope after sample cleaving. In the figures, the mark "*" represented the presence of etch-defects which were larger than 1×1 mm^2 under optical microscope having a 400X magnification (larger

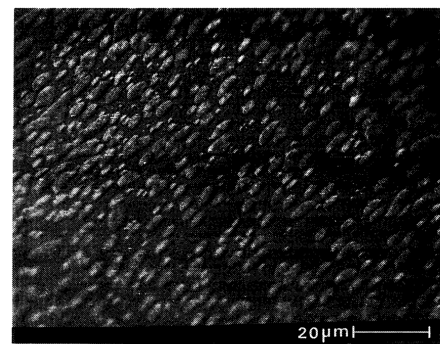

(a)

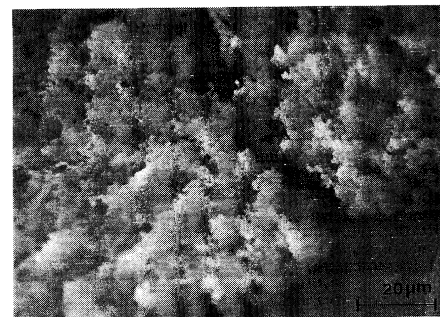

(b)

Fig. 7. Reaction products (a) and white residues (b) adhered on the etched surface.

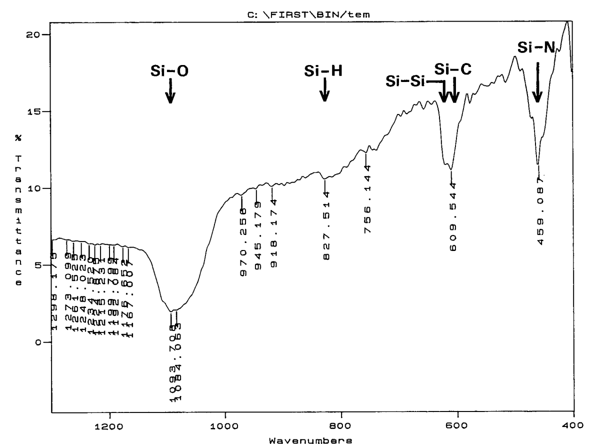

Fig. 8. FT-IR spectra of the white residues.

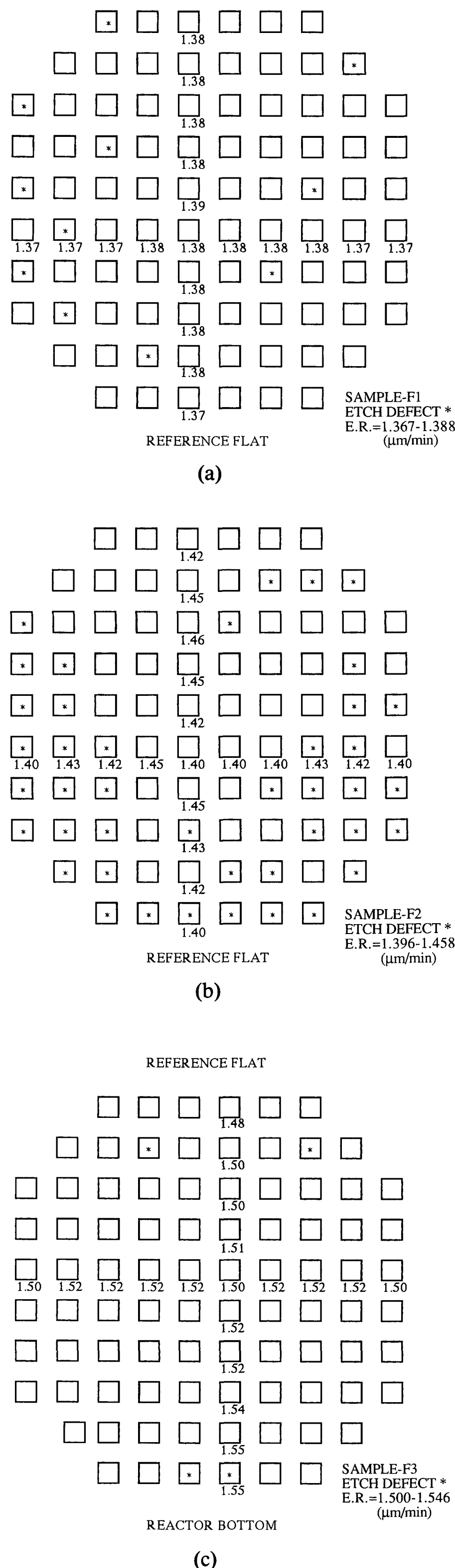

Fig. 9. Etch-defects and etch rate distributions for sample F1 (a), F2 (b), and F3 (c).

than 2.5 μm in reality). The existence probability of the defects for the sample F2 was about 48% and F1, F3 were 12%, 5% each. Also, the maximum deviation in the etch rate were measured Δ0.062, Δ0.046, and Δ0.021 μm/min for the sample F2, F3 and F1, respectively.

The defects in the sample F1 and F2 were radially distributed near the boundary of wafers. The phenomena could be explained for the sample F1, considering the liquid flow patterns in the deep cavity as shown in Fig. 10.[10-12] Because of the influence of the stirring bar rotating under the wafer, several trapped eddies were formed in the cavities located mainly near the edge like in Fig. 10(a) and these deteriorated the quality of the etched surface as mentioned previously. But the flow patterns were converted to the case shown in Fig. 10(b) near the center and so, the transfer of by-products to the outside were more feasible due to the convection of the etching solution. The active refreshment of solutions in the cavity made the surface quality improved. According to a report,[3] there might be some difference of the etch rates between the near-center and near-edge regions because the etch rate was mainly limited by mass transfer of reaction products and solution, but the effect was insignificant in our cases.

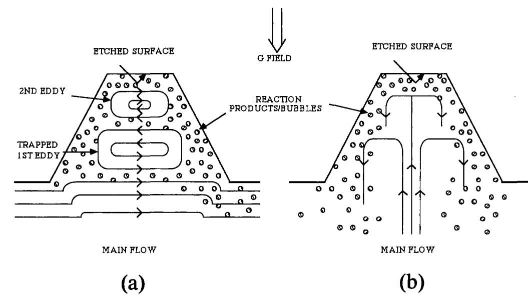

Fig. 10. Flow patterns in open cavities for the peripheral (a) and central (b) areas for sample F1.

Moreover, in the sample F1, as the acceleration field of gravity was directed toward the outside of cavity, the reaction products were easily transferred to the outside and therefore, the partial covering due to the evolved H_2 gas might act as a main factor in the defect generation.[10,15] But in case of sample F2, the field was directed toward the etched surface, that is, bottom of the cavity and so, the removal of by-products from the surface became more difficult. The surface quality was also improved near the center area as in the case of sample F1 and it was considered that the phenomena were caused not by the mass transfer through the flow patterns shown in Fig. 10(b) but by the natural out-diffusion of reaction products.[10]

Only a few defects were discovered for the case of sample F3. It could be inferred that there would not exist trapped eddies in the cavities, because the sample was placed perpendicularly to the solution and only gravity field and out-diffusion acted as transfer mechanisms. But under the circumstance there would be some variations in etch rates from the upper window to lower one. These might be originated from the unstable controlling in solution composition or temperature as we did our best.

The flatness of cavity surfaces where no defects were observed was investigated by a phase-contrast illumination (Nomarski method). The surfaces were flat in order of F3-F1-F2 as shown in Fig. 11. Especially for the case of sample F2, though the reaction products were out-diffused from the surface in proportion to "(diffusion coefficient in the solution x etching time)$^{1/2}$", their in-

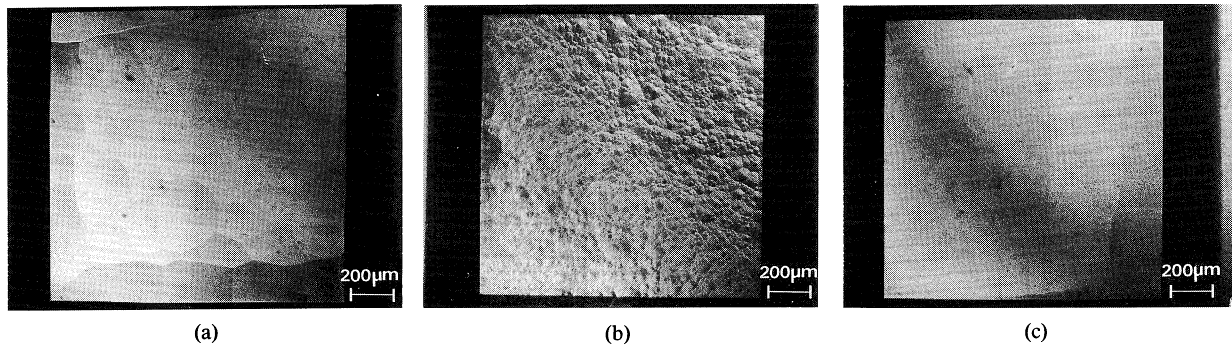

Fig. 11. Photographs of the etched surfaces under Nomarski mode for sample F1(a), F2(b), and F3(c).

fluence remained and deteriorated persistently the surface quality. Also the average etch depth in sample F3 was about 35 μm deeper than that in F1 and so, it could be assumed that the height and size of wavy textures became somewhat lower and larger.[9]

Finally, we carried out an additional etching experiment for non-mirror polished side of the wafers, in order to compare its etched surface with the one carried out on the mirror polished side and to investigate the possibility for the nondestructive thickness measurement of thin Si membranes. The sample B1 had the same specifications as the samples used in the previous experiment except that the oxide window patterns were formed on the backside of the wafer instead of front-side. And it was etched firstly for 240 min and secondly for 90 min more in the etching solutions having a posture of the case in sample F1.

After first and second etching, the existence probability of defects was about 19% and 26%, respectively as shown in Fig. 12. In the figure, the "**" marks represent newly-formed defects during second etching. For the firstly-etched sample, the defects were increased by $\Delta 7\%$ over the case of sample F1 and it could be caused by poor surface quality of sample B1. Also the increase in defect generation during secondly etching was due to the fact that the number of trapped eddies was increased as the cavity depth was deeper.

Next, the membrane thickness was measured nondestructively after the sample B1 was repeatedly etched with 1 min interval in etching solution. Figure 13 shows the measurement set-ups which was able to expose the membrane image with 50 watt tungsten lamp, and then examine the transmitted light with 50 magnification. This type of inspection had been carried out for the preparation of TEM specimens of 1 ~ 8 μm thick Si membranes.[16]

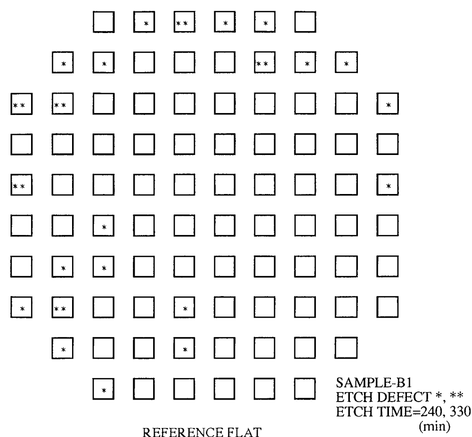

Fig. 12. Distribution of etch-defects for sample B1.

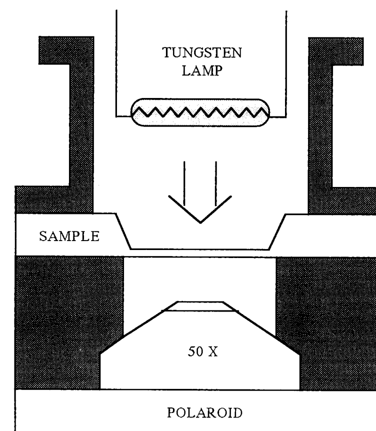

Fig. 13. Schematic drawing of the set-ups for transmitted light measurement.

There are two reasons for why we used a non-polished side instead of mirror side in this experimental. Firstly, the surface optimally etched by EPW solution showed a better surface uniformity than the non-mirror side of wafers. Thus we could obtain clearer transmitted light images for the membranes having a "mirror-polished surface and etched surface" due to less light dispersion, compared with the membrane having a "non-mirror polished surface and etched surface." Secondly, we also focused on the fact that in sensor processing the deep etching was typically done from the backside of Si wafer.

Figure 14 shows the transmitted light for the samples whose membrane thicknesses were 20 ~ 19, 15 ~ 13, 12 ~ 10, and 9 ~ 7 μm, respectively. Here the membrane thickness was measured through a 1000X magnified SEM observation of sample cross-section after transmitted light inspection. The light color was gradually changed from dark red to light yellow as the thickness was reduced. Also, the membrane had a convexed shape in which the boundary became thinner about 1 ~ 2 μm than the center region, especially, below the thickness range of 10

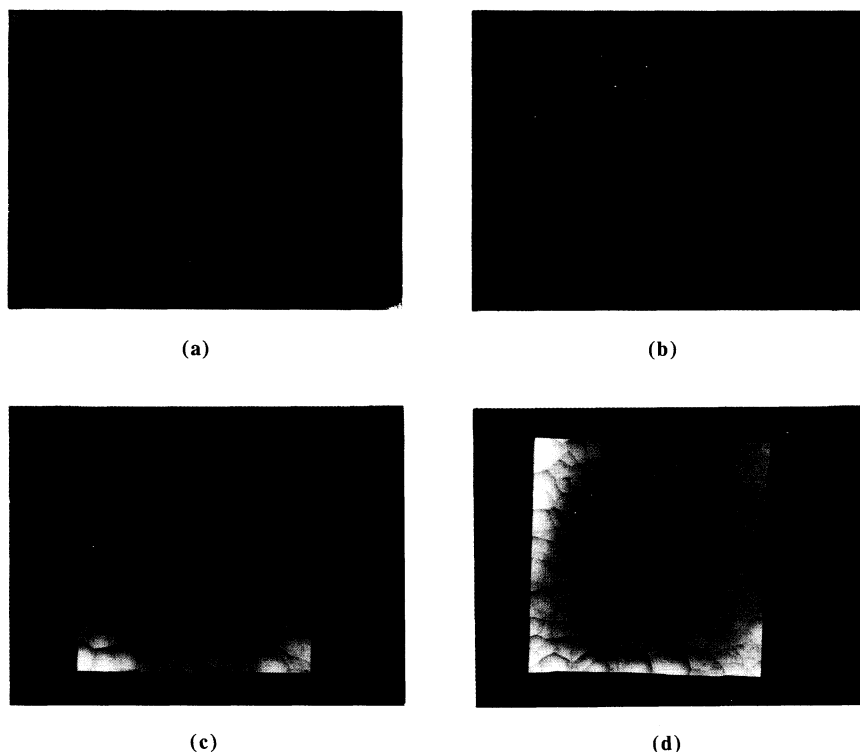

Fig. 14. Transmitted light colors through membrane having a thickness of 20 ~ 19(a), 15 ~ 13(b), 12 ~ 10(c), and 9 ~ 7 μm(d), respectively.

μm. This method was enable to measure the thickness within a permission error of $\Delta 1$ μm. If a monochromatic light source having a higher intensity was used in the apparatus, it would be proper method for the *invitro* thickness measurement during the batch fabrication of thin Si membranes.

§4. Conclusion

In conclusion, we knew that the characteristics of etched surface for the deep Si etching were closely related to the postures of the samples in the solution when the other etching conditions were fixed. And the more considerations were needed in order to obtain the membranes having a better surface quality and more uniform thickness by very deep etching using the standard Si wafers. The similar experiment and results for the deeper etching above 500 μm will be reported soon after, considering the batch fabrication of 20 μm thick or thinner membranes on 4-inch Si wafers.

Acknowledgements

We would like to thank M. B. Lee and S. W. Moon at KIST for SEM and FT-IR observation, respectively. Also, we are deeply indebted to I. K. Han and Y. H. Lee for their helpful discussions during the course of this work.

References

1) K. C. Lee: J. Electrochem. Soc. **137** (1990) 2556.
2) X.-P. Wu: Sens. Actuat. **9** (1986) 333.
3) M. Matsuoka, Y. Arai and Y. Yoshida: Jpn. J. Appl. Phys. **27** (1988) 784.
4) M. Mehregany and S. D. Senturia: Sens. Actuat. **13** (1988) 375.
5) A. Reisman, M. Berkenblit, S. A. Chan, F. B. Kaufman and D. C. Green: J. Electrochem. Soc. **126** (1979) 1406.
6) M. J. Declercq, L. Gerzberg and J. D. Meindl: J. Electrochem. Soc. **122** (1975) 545.
7) R. M. Finne and D. L. Klein: J. Electrochem. Soc. **114** (1967) 965.
8) F. Shimura: J. Electrochem. Soc. **127** (1980) 910.
9) E. Bassous and E. F. Baran: J. Electrochem. Soc. **125** (1978) 1321.
10) H. K. Kuiken and R. P. Tijburg: J. Electrochem. Soc. **130** (1983) 1722.
11) A. H. P. Skelland: *Diffusional Mass Transfer* (Wiley-Interscience, New York, 1974).
12) R. B. Bird, W. E. Stewart and E. N. Lightfoot: *Transfort Phenomena* (Wiley, New York, 1960).
13) T. Sugano: *Application of Plasma Processes to VLSI Technology* (Wiley-Interscience, New York, 1985) Chap. 2, p. 201.
14) R. C. Newman and R. S. Smith: J. Phys. Chem. Solids **30** (1969) 1493.
15) A. I. Stoller, R. F. Speers and S. Opresko: RCA Rev. **31** (1970) 265.
16) C. J. Varker and L. H. Chang: Solid State Technol. **146** (1983) 143.